

- 积分 $\int_a^b f(x) dx$: 矩形 \rightarrow 梯形 \rightarrow 样条 (Simpson方法)
- 方程 $y' = f(t, y) \rightarrow$ RK45方法 [高精度 $O(\Delta t^5)$]
- 方程 $\frac{\partial u}{\partial t} = a^2 \frac{\partial^2 u}{\partial x^2} \rightarrow$ Crank-Nicolson方法

基本引号: $u_i \leftarrow$ 空间坐标
 $u^n \leftarrow$ 时间坐标

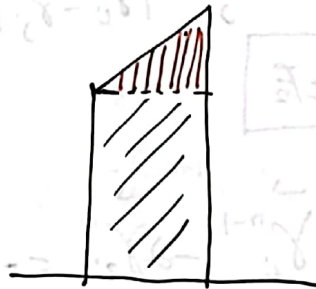
$$\frac{\partial u}{\partial t} = f(t, u)$$

$$\Leftrightarrow \frac{u^{n+1} - u^n}{\Delta t} = f(t^n, u^n)$$



OR

$$\frac{u^{n+1} - u^n}{\Delta t} = \frac{1}{2} [f(t^n, u^n) + f(t^{n+1}, u^{n+1})]$$



① f 为线性方程, 挪挪左边即可

② 非线性方程 \Rightarrow 自洽计算或采用最低级近似, 即

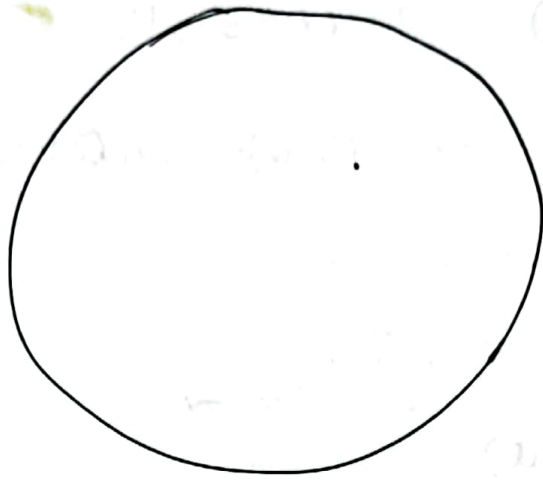
$$u^{n+1} = u^n + \frac{\Delta t}{2} [f(t^n, u^n) + f(t^{n+1}, \underbrace{u^n + \Delta t f(t^n, u^n)}_{\text{一级修正}})]$$

Lyapunov exponent is B stability

一级修正
即可。

应用 [德高] 方法不唯一, 当 N 很大时, 要考虑更多细节.

① 天体物理



存储,
精度 $O(h^n)$
复杂度...

本译程不考虑
它们。

$$m_i \ddot{\vec{r}}_i = -\sum_j \vec{F}_{ij}$$

$$F \sim \frac{G m_i m_j}{|\vec{r}_i - \vec{r}_j|^3} (\vec{r}_i - \vec{r}_j)$$

$$\ddot{\vec{r}}_i = -\sum_j \frac{G m_j}{|\vec{r}_i - \vec{r}_j|^3} (\vec{r}_i - \vec{r}_j)$$

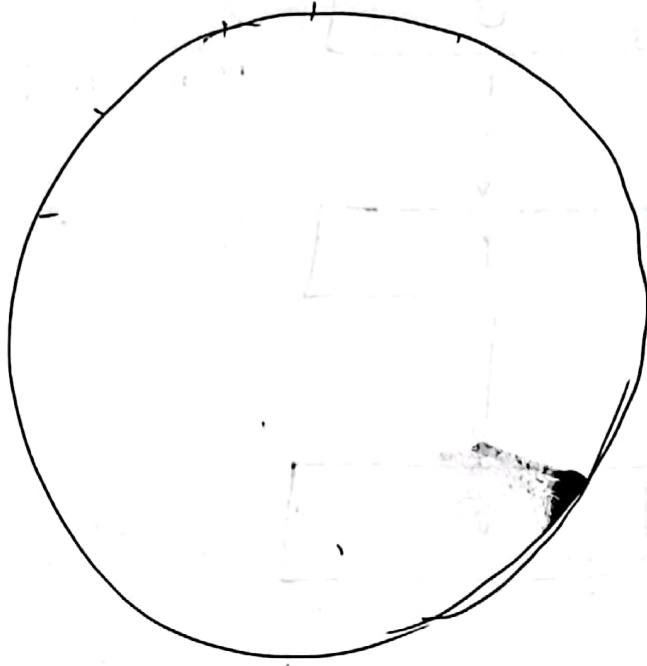
离散化后

$$\vec{r}_i^{n+1} + \vec{r}_i^{n-1} - 2\vec{r}_i^n = -\Delta t^2 \sum_j \frac{G m_j}{|\vec{r}_i^n - \vec{r}_j^n|} (\vec{r}_i^n - \vec{r}_j^n)$$

或

$$\vec{r}_i^{n+1} + \vec{r}_i^{n-1} - 2\vec{r}_i^n = -\frac{\Delta t^2}{2} \left(\begin{array}{l} \text{ⓐ } t^n \text{ 时刻的力} \\ + t^{n+1} \text{ 时刻的力} \end{array} \right)$$

② Kuramoto model



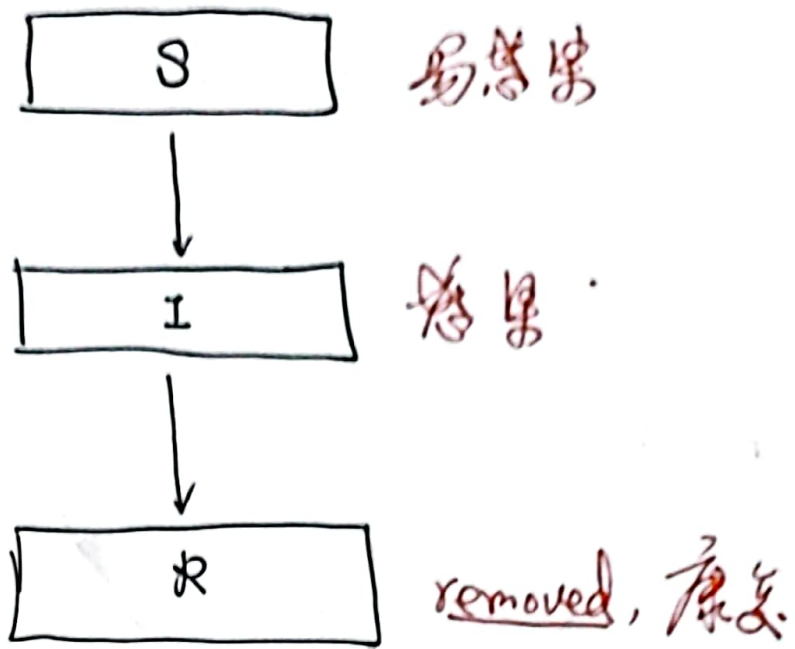
$$\dot{\theta}_i = \omega_i - \frac{k}{N} \sum_{j=1}^N \sin(\theta_i - \theta_j)$$

$$\theta_i^{n+1} - \theta_i^n = \Delta t \left[\omega_i - \frac{k}{N} \sum_{j=1}^N \sin(\theta_i^n - \theta_j^n) \right]$$

OR

$$\theta_i^{n+1} - \theta_i^n = \frac{\Delta t}{2} \left(t^n \text{ 时刻} + t^{n+1} \text{ 时刻} \right)$$

③ SIR model



$$\begin{cases} \dot{S} = -cSI \\ \dot{I} = cSI - gI \\ \dot{R} = gI \end{cases}$$

$$\Leftrightarrow \begin{cases} S^{n+1} = S^n - c\Delta t(S^n I^n) \\ I^{n+1} = I^n + (cS^n I^n - gI^n)\Delta t \\ R^{n+1} = R^n + gI^n\Delta t \end{cases}$$

④ Lorenz eq (1963)

Hendrik Lorentz 1853 - 1928 物理学家
Edward Lorenz 1917 - 2008 数学家, 气象学家

$$\begin{cases} \frac{dx}{dt} = \sigma(y - x) \\ \frac{dy}{dt} = x(\rho - z) - y \\ \frac{dz}{dt} = xy - \beta z \end{cases}$$

$$\begin{cases} X^{n+1} = X^n + \sigma \delta t (y^n - X^n) \\ Y^{n+1} = y^n + (X^n(\rho - z^n) - y^n) \delta t \\ Z^{n+1} = z^n + (X^n y^n - \beta z^n) \delta t \end{cases}$$

OR 时间平均..

⑤ Logistic map 与分叉理论 (bifurcation)

$$X_{n+1} = 4\lambda X_n (1 - X_n)$$

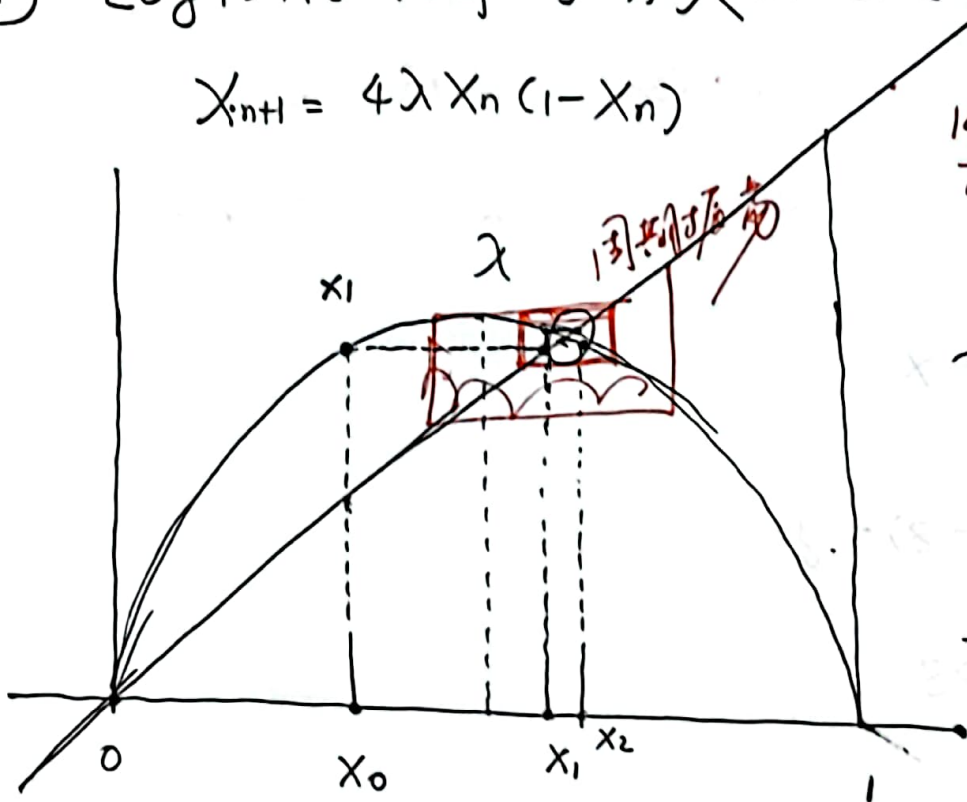
1845年 韦吕勒 Verhulst
指出人口变化模型

$$\frac{dx}{dt} = r x (1 - x)$$

可能 chaos.

单峰映射

以及 Feigenbaum 表



~~$X_{n+1} = 4\lambda X_n + 4\lambda X_n (1 - X_n)$~~

$$\frac{dx}{dt} = 4\lambda x(1-x) - x = 0 \quad \text{at } \begin{cases} x=0 \\ x = \frac{4\lambda-1}{4\lambda} \end{cases}$$

Near $x^* = 0 \Rightarrow$

$$\frac{dy}{dt} = 4\lambda y - y = (4\lambda - 1)y$$

Near $x^* = \frac{4\lambda-1}{4\lambda} \Rightarrow$

$$\frac{dy}{dt} = y(1 - 4\lambda)$$

相反

The Bak-Tang-Wiesenfeld sandpile model around the upper critical dimension

S. Lübeck* and K. D. Usadel†

*Theoretische Tieftemperaturphysik, Gerhard-Mercator-Universität Duisburg,
Lotharstr. 1, 47048 Duisburg, Germany*

(Received 19 June 1997)

We consider the Bak-Tang-Wiesenfeld sandpile model on square lattices in different dimensions ($D \leq 6$). A finite size scaling analysis of the avalanche probability distributions yields the values of the distribution exponents, the dynamical exponent, and the dimension of the avalanches. Above the upper critical dimension $D_u = 4$ the exponents equal the known mean field values. An analysis of the area probability distributions indicates that the avalanches are fractal above the critical dimension.

PACS number: 05.40.+j

I. INTRODUCTION

Bak, Tang and Wiesenfeld [1] introduced the concept of self-organized criticality (SOC) and realized it with the so-called 'sandpile model' (BTW model). The steady state dynamics of the system is characterized by the probability distributions for the occurrence of relaxation clusters of a certain size, area, duration, etc. In the critical steady state these probability distributions exhibit power-law behavior. Much work has been done in the two dimensional case. Dhar introduced the concept of 'Abelian sandpile models' which allows to calculate the static properties of the model exactly [2], e.g. the height probabilities, height correlations, number of steady state configurations, etc [2-5]. Recently, the exponents of the probability distribution which describes the dynamical properties of the system were determined numerically [6]. On the other hand both mean field solutions (see [7] and references therein) and the solution on the Bethe lattice [8] are well established and both yield identical values of the exponents. The mean field approaches are based on the assumption that above the upper critical dimension D_u the avalanches do not form loops and the avalanches propagation can be described as a branching process [9]. Despite various theoretical and numerical efforts the value of D_u is still controversial. In an early work, Obukhov predicted $D_u = 4$ using an ϵ -expansion renormalization group scheme [10]. Later Diaz-Guilera performed a momentum space analysis of the corresponding Langevin equations which confirmed $D_u = 4$ [11]. Grassberger and Manna concluded from numerical investigations of the BTW model in $D \leq 5$ the same result [12]. In contrast, comparable simulations and the similarity to percolation led several authors to the conjecture that $D_u = 6$ [13] comparable to the related forest fire model of Drossel and Schwabl (see [14] for an overview).

In the present work we consider the BTW model in various dimensions ($D \leq 6$) on lattice sizes which are significant larger than those considered in previous works [12,13,15]. A finite size scaling analysis allows us to determine the avalanche exponents, the dynamical exponent and to analyse whether the avalanche clusters are fractal. Our analysis reveals that the upper critical dimension is $D_u = 4$ and that the avalanches display a fractal behavior above D_u . We discuss the dimensional dependence

of the exponents and derive scaling relations. Finally we briefly report results of similar investigations of the D -state model which is a possible generalization of the two-state model introduced by Manna in two-dimensions [16]. It is known that the BTW model and Manna's model belong to different universality classes in $D = 2$ [15,6].

II. MODEL AND SIMULATIONS

We consider the D -dimensional BTW model on a square lattice of linear size L in which integer variables $h_r \geq 0$ represent local heights. One perturbs the system by adding particles at a randomly chosen site h_r according to

$$h_r \mapsto h_r + 1, \quad \text{with random } r. \quad (1)$$

A site is called unstable if the corresponding height h_r exceeds a critical value h_c , i.e., if $h_r \geq h_c$, where h_c is given by $h_c = 2D$. An unstable site relaxes, its value is decreased by h_c and the $2D$ next neighboring sites are increased by one unit, i.e.,

$$h_r \rightarrow h_r - h_c \quad (2)$$

$$h_{nn,r} \rightarrow h_{nn,r} + 1. \quad (3)$$

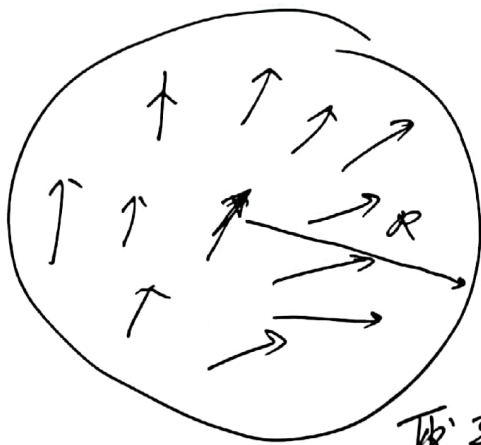
In this way the neighboring sites may be activated and an avalanche of relaxation events may take place. The sites are updated in parallel until all sites are stable. Then the next particle is added [Eq. (1)]. We assume open boundary conditions with heights at the boundary fixed to zero.

System sizes $L \leq 256$ for $D = 3$, $L \leq 80$ for $D = 4$, $L \leq 36$ for $D = 5$, and $L \leq 18$ for $D = 6$ are investigated. Starting with a lattice of randomly distributed heights $h \in \{0, 1, 2, \dots, h_c - 1\}$ the system is perturbed according to Eq. (1) and Dhar's 'burning algorithm' is applied in order to check if the system has reached the critical steady state [2]. Then we start the actual measurements which are averaged over at least 2×10^6 non-zero avalanches. We studied four different properties characterizing an avalanche: the number of relaxation events s , the number of distinct toppled lattice site s_d (area), the

⑦ Flocking behavior / Collective behavior

Vissek model

$$\underline{r}_i^{t+\delta t} = \underline{r}_i^t + \delta t v_0 (\underline{S}_i^{t+\delta t})$$



取平均速度

or $\underline{v}_i^{n+1} = \underline{v}_i^n + \delta t \underline{V}_i^{n+1}$

$$\underline{V}_i^{n+1} = \left(\sum_{|\underline{r}_i - \underline{r}_j| \leq R} \underline{v}_j^n \right) / N$$

⑧

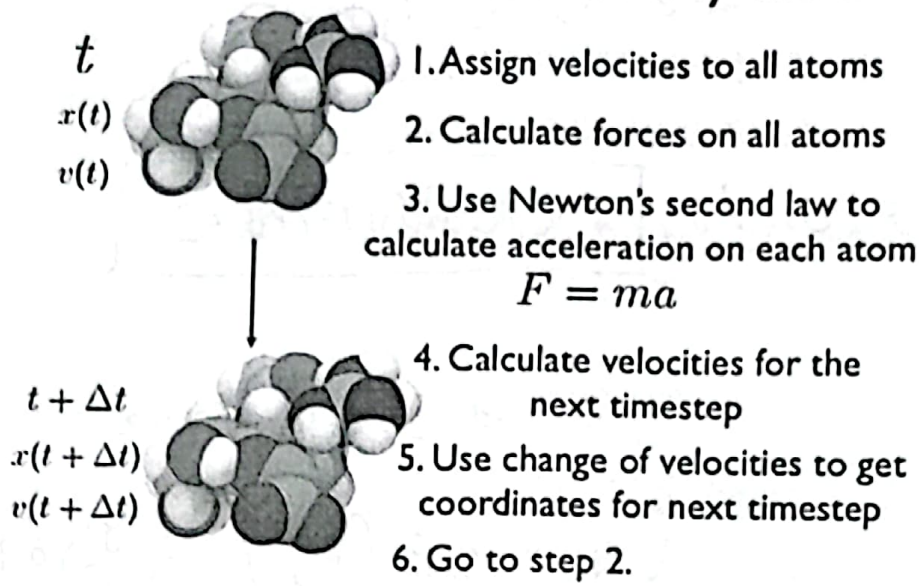
or $\underline{v}_i^{n+1} = \text{平均速度} + \sum_i^t \text{fluctuation.}$

其中 $\langle \xi_i^t \xi_j^{t'} \rangle = \sigma^2 \delta_{t+t'} \delta_{ij}$ 是 white noise.

- 有许多不同方法定义 \underline{v}_i^{n+1} , 它们可能给出不同而/相同的结果。

8

Molecular Dynamics



应用最广泛

- ① 求 $E \rightarrow$ 最小值 (结构)
- ② 求 eq of motion (反应)

- ① 第一性原理
- ② 材料
- ③ 分子生物学 / 结构学
- ⋮

本质上和行卷一样，因为人数众多，也
 开发了许多不同的方法。

$$L = \frac{1}{2} \sum_i m_i \vec{v}_i^2 - \sum_{i,j} U(\vec{x}_i - \vec{x}_j)$$

问题: 如何定义 $U(\vec{x})$, 不可各向同性吧?

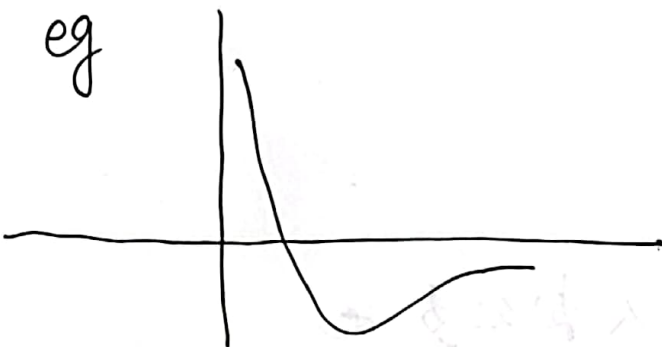


Lennard-Jones potential

$$V(r) = 4\epsilon \left[\left(\frac{\sigma}{r}\right)^{12} - \left(\frac{\sigma}{r}\right)^6 \right]$$



方势



Morse potential

$$\underline{V_0 \left(1 - e^{-\alpha(r-r_e)}\right)^2}$$

Verlet 算法

$$\vec{X}_i(t+\Delta t) + \vec{X}_i(t-\Delta t) = 2\vec{X}_i(t) + \vec{X}_i''(t)\Delta t^2 + o(\Delta t^4)$$

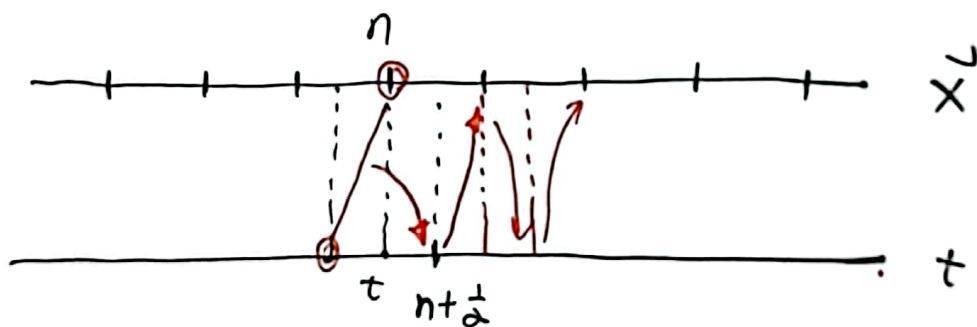
力
" \vec{f}_i/m_i

$$\vec{X}_i(t+\Delta t) = 2\vec{X}_i(t) - \vec{X}_i(t-\Delta t) + \frac{\vec{f}_i}{m_i}\Delta t^2 + o(\Delta t^4)$$

求 Velocity

$$\vec{V}_i(t) = \frac{1}{\Delta t} [\vec{X}_i(t+\Delta t) - \vec{X}_i(t-\Delta t)] + o(\Delta t^2)$$

leap frog 算法



$$\vec{V}_i(t + \frac{\Delta t}{2}) = \vec{V}_i(t - \frac{\Delta t}{2}) + \frac{\vec{f}_i(t_0)}{m_i}\Delta t + o(\Delta t^3)$$

$$\vec{X}_i(t + \Delta t) = \vec{X}_i(t_0) + \vec{V}_i(t_0 + \frac{\Delta t}{2})\Delta t + o(\Delta t^3)$$

Beeman 算法

$$\begin{cases} \vec{X}_i(t+\Delta t) = \vec{X}_i(t) + \vec{V}_i(t)\Delta t + \frac{4f_i(t) - f_i(t-\Delta t)}{m_i} \frac{\Delta t^2}{6} \\ V_i(t+\Delta t) = V_i(t) + \frac{2f_i(t+\Delta t) + 5f_i(t) - f_i(t-\Delta t)}{m_i} \frac{\Delta t}{6} \end{cases}$$

更复杂的算法，以期进一步提高精度。

Evolution of Schrödinger eq

(9)

$$i \frac{\partial}{\partial t} \psi = H(t) \psi$$

$$\psi | \psi \rangle = \sum_n C_n | \varphi_n \rangle$$

$$i \dot{C}_n = \sum_m t_{nm} C_m$$

or

$$C_n(t+\Delta t) = C_n(t) + i \Delta t \sum_m t_{nm} C_m(t)$$

这称为 eq of motion method!

Maxwell eq 不讲, 以后专门讨论.

Kicked rotor and Anderson localization

Boulder School on Condensed Matter Physics, 2013

Dominique Delande
*Laboratoire Kastler-Brossel, Université Pierre et Marie Curie,
 Ecole Normale Supérieure, CNRS; 4 Place Jussieu, F-75005 Paris, France*

CONTENTS

Introduction: Anderson localization	1
I. Lecture I: The periodically kicked rotor	1
II. Lecture II: Experiments with the periodically kicked rotor	1
III. Lecture III: The quasi-periodically kicked rotor	1
A. The model	1
B. The periodically kicked pseudo-rotor	2
C. Anderson transition	3
D. Finite-time scaling	5
E. Universality	6
F. Self-consistent theory of localization	6
G. Perspectives	8
References	9

INTRODUCTION: ANDERSON LOCALIZATION

I. LECTURE I: THE PERIODICALLY KICKED ROTOR

II. LECTURE II: EXPERIMENTS WITH THE PERIODICALLY KICKED ROTOR

III. LECTURE III: THE QUASI-PERIODICALLY KICKED ROTOR

A. The model

How can the kicked rotor be used to study Anderson localization in more than one dimension? The first idea is to use a higher-dimensional rotor with a classically chaotic dynamics and to kick it periodically. It turns out that this is not easily realized experimentally, as it requires to build a specially crafted spatial dependence [1]. Yet, remember that time and space have switched roles, and so a simpler idea is to use additional temporal dimensions rather than spatial dimensions. Instead of kicking the system periodically with kicks of constant strength, one may use a temporally quasi-periodic excitation. Various schemes have been used [2], but the one allowing to map on a multi-dimensional Anderson model uses a quasi-periodic modulation of the kick strength, the kicks being applied at fixed time interval [3].

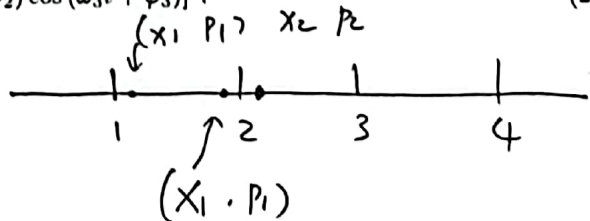
We will be interested in a 3d Anderson model, obtained by adding two quasi-periods to the system: [27]

$$X_{n+1} = X_n + \int_n^{n+1} \dot{X} dt = \frac{p^2}{2} + K(t) \cos x \sum_n \delta(t-n), \quad (1)$$

with

$$K(t) = K [1 + \epsilon \cos(\omega_2 t + \varphi_2) \cos(\omega_3 t + \varphi_3)] \quad (2)$$

$$\begin{cases} \dot{X} = \frac{\partial H}{\partial p} = p \\ \dot{p} = -K \sin x \sum_n \delta(t-t_n) \end{cases}$$



It is easy to write the classical evolution from kick n to kick $n + 1$, exactly as we did for the periodically kicked rotor. One obtains:

$$\begin{cases} p_{n+1} = p_n + \mathcal{K}(n) \sin x_n \\ x_{n+1} = x_n + p_{n+1} \end{cases} \quad (3)$$

that is the same result than for the periodically kicked rotor, except that \mathcal{K} now depends quasi-periodically on time.

Now where is the three dimensional aspect in this problem? The answer lies in a mapping of this quasi-periodic kicked rotor on a 3d kicked "pseudo"-rotor with the special initial condition of a "plane source", as follows.

B. The periodically kicked pseudo-rotor

Let us consider a 3d periodically kicked pseudo-rotor, whose Hamiltonian is:

$$\mathcal{H} = \frac{p_1^2}{2} + \omega_2 p_2 + \omega_3 p_3 + K \cos x_1 [1 + \varepsilon \cos x_2 \cos x_3] \sum_n \delta(t - n), \quad (4)$$

This is not a true rotor, because of the unusual form of the kinetic energy in directions 2 and 3, where it is a linear – instead of quadratic – function of the momentum, hence the name pseudo-rotor. Being a periodic system, we can again write the map over one period:

$$\begin{aligned} p_{1_{n+1}} &= p_{1_n} + K \sin x_{1_n} (1 + \varepsilon \cos x_{2_n} \cos x_{3_n}), \\ p_{2_{n+1}} &= p_{2_n} + K \varepsilon \cos x_{1_n} \sin x_{2_n} \cos x_{3_n}, \\ p_{3_{n+1}} &= p_{3_n} + K \varepsilon \cos x_{1_n} \cos x_{2_n} \sin x_{3_n}, \\ x_{1_{n+1}} &= x_{1_n} + p_{1_{n+1}}, \\ x_{2_{n+1}} &= x_{2_n} + \omega_2, \\ x_{3_{n+1}} &= x_{3_n} + \omega_3. \end{aligned} \quad (5)$$

The last two equations are trivially integrated: $x_{2_n} = x_{2_0} + n\omega_2$ and similarly for x_3 . If we now start with the initial condition $x_{2_0} = \varphi_2, x_{3_0} = \varphi_3$, it is straightforward to realize that the mapping for p_1 and x_1 is *exactly* the same than the mapping (3) of the quasi-periodically kicked rotor. In other words, the classical dynamics of the kicked pseudo-rotor along the direction 1 is strictly identical to the one of the quasi-periodically kicked rotor.

The same mapping exists for the quantum evolution. Consider the evolution of a wavefunction Ψ with the initial condition

$$\Psi(x_1, x_2, x_3, t = 0) \equiv \psi(x_1, t = 0) \delta(x_2 - \varphi_2) \delta(x_3 - \varphi_3). \quad (6)$$

This initial state, perfectly localized in x_2 and x_3 and therefore entirely delocalized in the conjugate momenta p_2 and p_3 , is a "plane source" in momentum space [1]. A simple calculation shows that the stroboscopic evolution of Ψ under (4) coincides exactly with the evolution of the initial state $\psi(x = x_1, t = 0)$ under the Hamiltonian (1) of the quasi-periodically kicked rotor (for details, see [5]). An experiment with the quasi-periodic kicked rotor can thus be seen as a localization experiment in a 3d disordered system, where localization is actually observed in the direction perpendicular to the plane source. In other words, the situation is comparable to a transmission experiment where the sample is illuminated by a plane wave and the exponential localization is only measured along the wave vector direction. Therefore, the behavior of the quasi-periodic kicked rotor (1) matches *all* dynamic properties of the quantum 3d kicked pseudo-rotor.

For sufficiently large K and not too small ε , the classical dynamics of the pseudo-rotor is a chaotic diffusion in momentum space. Indeed, coupling to the strongly chaotic direction 1 is sufficient to make the dynamics along directions 2 and 3 also diffusive [6]. However, the diffusion tensor is not isotropic. It can be computed like for the periodically kicked rotor, that is assuming no position-momentum correlation and complete delocalization in configuration space. One obtains for the anisotropic diffusion tensor (for ε smaller than unity):

$$D_{11} \approx (K^2/4)(1 + \varepsilon^2/4), \quad (7)$$

$$D_{22} \approx K^2 \varepsilon^2 / 16, \quad (8)$$

$$D_{33} \approx K^2 \varepsilon^2 / 16, \quad (9)$$

$$D_{i \neq j} \approx 0. \quad (10)$$